ZIBELINE INTERNATIONAL™ PUBLISHING

Pakistan Journal of Geology (PJG)

DOI: http://doi.org/10.26480/pjg.01.2022.15.23

ISSN: 2521-2915 (Print)
ISSN: 2521-2923 (Online)
CODEN: PJGABN

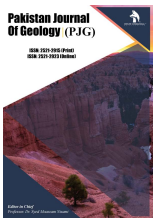

RESEARCH ARTICLE

USE ELECTRICAL RESISTIVITY METHOD TO INFER SUBSURFACE LITHOLOGY USING DEPTH SLICING APPROACH: A CASE STUDY OF ORER0KPE, DELTA STATE NIGERIA

Star Otitie Umayah

Department of Physics, Faculty of Science Delta State University, Abraka Nigeria.
****Corresponding Author Email: Otitiestarumayah@gmail.com***

ARTICLE DETAILS

Article History:

Received 26 February 2022
Accepted 28 March 2022
Available online 04 April 2022

ABSTRACT

The goal of this research is to use vertical electrical sounding to analyze the underlying lithological layers of Orerokpe, Delta State, Nigeria. The Schlumberger configuration with a maximum electrode spacing of 200 m was used in 15 VES surveys for the investigation. The data were acquired using ABEM SAS 4000 Terrameter and processed using the WINRESIST program. The data collected were analyzed and interpreted in both qualitative and quantitative terms. Distribution of the resistivity values at different depths are represented by iso-resistivity and electrical profile maps for different electrode spacing, AB at 2 m, 3 m, 4 m, 6 m, 6m (repeated), 9 m, 12m, 15m, 15m (repeated), 20m, 25m, 32m, 40m, 40m (repeated), and 50 m respectively. Results obtained from the study area revealed that geoelectric layers range from 3 to 4. Further findings from the study revealed that the iso-resistivity plot of AB/2 at various depths, it was observed that the area is predominantly underlain with coarse, medium, and fine sand as AB/2 increases.

KEYWORDS

Apparent depth, resistivity, Sand, Clay, Nigeria.

1. INTRODUCTION

For decades, the electrical resistivity method has been utilized in conjunction with borehole data, investigations to infer subsurface lithology (Chukwuma, et al., 2015). It has recently been employed in environmental surveys. To quickly determine the nature of water-bearing layers, geophysical research approaches such as geo-electric, electromagnetic, seismic, and geophysical borehole logging are available (Alile, et al. 2008). The type, porosity, water content, and density of the subsurface condition can all be determined through surface investigation. This is usually accomplished through the use of the earth's electrical and seismic characteristics and without the need for any ground drilling. In a simple geological environment with horizontal or near horizontal layering and lateral homogeneity, the vertical electrical sounding (VES) technique of the electrical resistivity method is useful in subsurface layer delineation and layer thickness or depth to geoelectric interface determination and is thus widely used in engineering site and groundwater investigations in both sedimentary and basement environments (Eyankware, et al., 2022; Olorunfemi and Fasuyi 1993; Eyankware and Umayah, 2022; Edet and Okereke 1997; Eyankware, et al., 2021; Ajayi et al., 2005; Umayah and Eyankware, 2022; Olorunfemi et al., 2005; Eyankware, et al., 2020). Similarly, in Nigerian sedimentary and basement terrain, the 1D VES method has been adopted to determine subsurface lithology, aquifer vulnerability, and water-bearing units (Eyankware, et al., 2022; Eyankware and Aleke, 2021; Umayah and Eyankware, 2022; Eyankware, 2019). The 1D VES technique involves gradually extending the current (A, B) and potential (M, N) electrodes with respect to a fixed center of the electrode array to assess vertical variations in ground resistivity. Similarly, this method has been used to infer subsurface lithology using accessible lithologic logs from the area of interest (Oli et al., 2020; Eyankware et al., 2020; Eyankware et al., 2022). The electrical resistivity approach was employed to further delineate subsurface lithology within the study region, with the use of iso-resistivity acquired from VES point at present electrode spacing.

2. PHYSIOGRAPHY AND GEOGRAPHICAL LOCATION

The study area is located between latitudes 5°32'0" N and 5°44'0" N, and longitudes 5°54′E and 5°46'0" E - 6°0'0" E, as shown in Figure 1. Orerokpe is also part of the Sombreiro-Warri Deltaic Plain, a low-lying physiographic province with rain virtually all year and a mean daily temperature of 31.2°C (NMA, 2003).

3. GEOLOGY/HYDROGEOLOGY

The Niger Delta's sedimentary ecosystems and morphological features have been thoroughly investigated (Short and Stauble, 1967; Allen, 1965; Allen, 1970; Durotoye, 1989; Odemerho and Ejemeyovwi, 2007). The Sombreiro-Warri Deltaic Plain deposits, which conformably overlie the Benin Formation, the youngest of the three major formations that make up the Niger Delta Basin's sedimentary fill, are underlain by the Quaternary Sombreiro-Warri Deltaic Plain deposits. The Benin Formation is made up of massive continental/fluvial sands and gravels. The Agbada Formation, which consists of paralic sands and shales, and the base Akata Formation, which consists of holomarine shales, silts, and clays, are older formations that are only found in the subsurface (Short and Stauble, 1967; Amajor, 1990). the Eocene-Oligocene Ogwashi Asaba Formation and the Ameki Formation are both Eocene-Oligocene in age. The sands and clays of the Sombreiro-Warri Deltaic Plain are one of four Quaternary-Holocene deposit suites that hide the Benin Formation in the western Delta, the others being the beach ridges, freshwater swamps, and brackish water/Mangroove Swamps. These deposits have not been given formal names because they are commonly acknowledged as current expressions and continuations of the Benin Formation. These sands, sandy clays, silts, and subordinate, lensoid clay bands are thought to have been deposited

Quick Response Code	Access this article online	
	Website: www.pakjgeology.com	**DOI:** 10.26480/pjg.01.2022.15.23

during interglacial marine transgressions during the Quaternary (Durotoye, 1989). According they're made up of fluvial/tidal channel sediments, tidal flats, and mangrove swamp deposits (Short and Stauble, 1967). The sands are micaceous and feldspathic, with a roughness that ranges from sub-rounded to angular, and they create excellent aquifers. However, because to rapid horizontal and vertical facies changes, occurrence depths and thicknesses are unpredictable and may not be correctly anticipated at individual sites, either within the study region or throughout the Sombreiro-Warri Deltaic Plain, as illustrated in Fig.1. Most water-bearing units in the research region, according to are semi-confined and exist at depths ranging from 45 to 212 meters (Aweto, 2013; Akpoborie, et al., 2000).

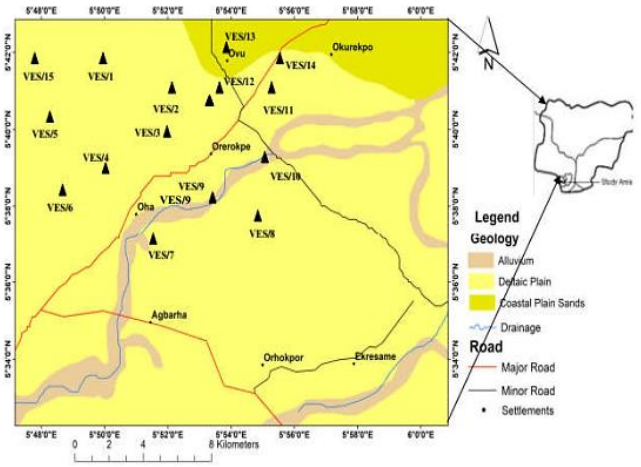

Figure 1: Geology Map of the study area. Source modified after (Umayah and Eyankware, 2022)s

4. METHOD

4.1 Vertical Electrical Sounding (VES)

The earth's resistance was measured using the Abem Terrameter SAS 1000, and a total of fifteen (15) VES were conducted using the Schlumberger configuration, with electrode spacing (AB) ranging from 2 to 200 m and potential electrode spacing (MN) ranging from 0.52 m to 7.00 m. For each electrode separation, the electrical resistances were multiplied by the relevant geometric factor (k) to determine apparent resistivity. The smoothed curves were first qualitatively interpreted with master curves and standard charts and then processed with the computer modeling WINRESIST program (Orellana and Moonney, 1966; Eyankware, 2015). At various VES locations, the displayed curves automatically revealed the number of layers, thickness, depth, and average resistivity for each layer. For each VES location, the Global Positioning System (GPS) was used to obtain accurate coordinates and elevation data.

$$\rho a = KR \quad (1)$$

where ρa is an apparent resistivity and the earth resistance (R) is given as

$$R = \Delta V / I \quad (2)$$

The geometric factor k is represented as as $K = \frac{\pi(AB)^2-(MN)^2}{MN}$ (3)

4.2 VES survey

The summary of the interpreted VES survey is presented in Table 1. Findings from VES revealed geoelectric layers range from three to six layers with different intra-facies and inter-facies changes as shown in Table 1.

4.3 Iso-Resistivity Plots of the study area

At specified AB/2 intervals, an iso-resistivity map was generated using the Golden Surfer 11.0 version. 2 m, 3 m, 4 m, 6 m, 6m (repeated), 9 m, 12m, 15m, 15m (repeated), 20m, 25m, 32m, 40m, 40m (repeated), and 50 m as shown in Fig. 2a to 2o. It depicts the color spectrum that corresponds to earth material resistivity values. Iso-resistivity maps, according to Mbonu et al. (1991), are a qualitative analysis tool that exposes possible variations in resistivity with depth at specified electrode spacing across a specific area, but they do not give the true resistivity of a single geo-electrical layer or unit. Because the effective depth of transmission is considered to be approximately 2/3 of the current electrode spacing (AB/2).

Table 2: Resistivity value of rock within the study area. After (Aweto, and Akpoborie, 2015)

S/No	Resistivity range	Rock type
1	42.3-82.4	Clay
2	202.5 -1402.2	Coarse sand
3	505.1 – 917.6	Medium sand
4	527.0 – 1207.0-∞	Fine sand

4.4 Iso-resistivity map (AB/2 at 2 m)

At a depth of 2 m, the iso-resistivity strength AB/2 contour map suggested a depth close to topsoil (Figure 2a). The purple color and resistivity value of 0 to about 500 m in the southeast of the study region could imply clay and sand (Figure 2a and Table 2). The southwest half of the research area, with resistivity values ranging from 2500 to approximately 7500 m, can be interpreted as fine sand and coarse sand, respectively. The AB/2m at 2m revealed that the area is underlain by sand, according to the findings in Figure 2a.

4.5 Iso-resistivity map (AB/2 at 3 m)

In Fig. 2b, the AB/2 contour map of iso-resistivity strength at 9 m revealed that the majority of the study area had a high resistivity value. As illustrated in Figure 2b, the high resistivity values span from 500 to about 6500 m, with green, yellow, and red colors. These high resistivity values denote that at 3 the subsurface is underlain by fine, coarse, and medium sand respectively. While low resistivity values 0 to approximately 500 Ωm were noticed in some parts of NE and selected parts of SE as shown in Figure 2b. Low resistivity value is an indication that the aforementioned areas are underlain by sand and clay as shown in Figure 2b.

4.6 Iso-resistivity map (AB/2 at 4 m)

The AB/2 contour map of iso-resistivity strength at 4 m in Figure 2c showed resistivity value decreases with relatively high resistive material underlay the SE, SW, and slightly some selected part of NE area as shown in Figure 2c. With resistivity values of 600 to approximately 3000 Ωm, The resistivity ranges shown by blue, green, yellow, and white may indicate coarse, medium, and fine sand respectively as shown in Figure 2c. While areas with low resistivity values of 0 to 82.4 Ωm, with dark blue colour may indicate area underlain by clay (Figure 2c).

4.7 Iso-resistivity map (AB/2 at 6 m)

In Figure 2d, the AB/2 contour map of iso-resistivity strength at 6 m demonstrated that the resistivity trend increased slightly when compared to AB/2 at 4 m. According to Figure 2d, a major portion of the land had a high resistivity value ranging from 200 to 3600 m, with blue, green, yellow, red, and white colors. This may indicate that the area is underlain by coarse, medium, and fine sand respectively see Figure 2d. While low resistivity values of 0 to approximately 190 Ωm was observed in some selected part of NW and NE, this may be an indication that such area is underlain by clay (Figure 2d).

4.8 Iso-resistivity map (AB/2 at 6 m repeated)

The AB/2 contour map of iso-resistivity strength at 6 m (repeated) in Figure 2e below shows that relatively high resistive materials underlay the NW, SW, and SE parts of the study area, with resistivity values ranging from 500 m to approximately 9500 m in purple, green, red, and yellow, which may indicate sections underlain by coarse, medium, and fine sand. Further observations from Figure 2e revealed that the light purple color and resistivity value of 0 to roughly 500 m in the SE, NE, and selected sections of NW may imply that the aforementioned area is underlain by sand and clay.

4.9 Iso-resistivity map (AB/2 at 9 m)

The AB/2 contour map of iso-resistivity strength at 9 m in Figure 2f showed resistivity value decreases with relatively high resistive material underlay the SW, NE, and SE parts of the study area in light purple, red, yellow, green, and blue color with a resistivity value range of 500m to approximately 6500m may indicate area underlain by coarse medium, and fine sand (Figure 2f). Low resistive value was observed in selected parts of NW, NE, and SW in light purple with resistivity value of 0 to approximately 500 Ωm, may be interpreted as area underlain by clay/sand (Figure 2f).

Table 1: Iso-resistivity modeling of resistivity across the study area

Sampling Code	AB/2= 1 m	AB/2= 2 m	AB/2 = 3 m	AB/2 = 4 m	AB/2 = 6 m	AB/2 = 6 m (R)	AB/2 = 9 m	AB/2 = 12 m	AB/2 = 15 m	AB/2 = 15 m (R)	AB/2 = 20m	AB/2 = 25 m	AB/2 = 32m	AB/2 = 40m	AB/2 = 40m (R)	AB/2 = 50m
VES/01	1090	1500	2768	1321	1104	9324	655	905	820	1785	3436	7230	6358			
VES/02	690	800	1135	2148	1674	1807	1400	5283	1351	945	701	511	1359	1230	700	
VES/03	588	838	889	916	989	987	1273	2134	1500	1200	7466	2900	2052	2900		
VES/04	459	914	1034	977	797	798	709	516	300	298		534	585	742	830	947
VES/05	455.6	844.7	1045	1209	1739	1492	1350	1028	1214	899.7		3262	1082	1051	1912	2100
VES/06	1643	1100	6312	3000	3460	4200	6399	6000	6101	5000	3000					
VES/07	6436	7556	872	853	800	890	600	305	499	600	2700	850	1110	1490	799	817
VES/08	1633	1400	1317	1133	1262	1366	1516	1800	2200	1800		1576	1200	740	851	
VES/09	161	166	186	207	255	249	232	273	241	247		821	795	900	700	700
VES/10	1487	1200	1800	2801	1784		945	831	651	530			2580	1075	1100	1180
VES/11	280	202	293	400	874	732	1468	2501	3183	1553	3301	3181	6446	10256	3591	
VES/12	406	337	300	92.7	86	183	110	150	190	137	240	229	415	1280	2298	
VES/13	145	250	332	324	319	296	276	280	320	273	384	480	750	900	700	1660
VES/14	849	1450	1238	1225	1071	873	744	595	542	659	609	548	569	507	367	750
VES/15	38.3	18	19	27	20	57	81	95	130	110	140	273	190	230	856	1275

Where (R) is repeated

4.10 Iso-resistivity map (AB/2 at 12 m)

The AB/2 contour map of iso-resistivity strength at 12 m in Figure 2f, with high resistive values observed in the selected SW part of the area, a larger part of the iso-resistivity map of AB/2 at 12 m tends to have high resistive values range of 400 m to approximately 6000 m, with blue, green, yellow, and red, this could indicate coarse, medium, and fine sand (Figure 2g and Table 2). A resistivity value range of 0 m to about 400 m was detected in selected sections of the NW, SE, SW, and NE, which might be interpreted as a region underlain by clay/sand (Figure 2g).

4.11 Iso-resistivity map (AB/2 at 15 m)

In Figure 2h, the AB/2 contour map of iso-resistivity strength at 15 m shows relatively high resistive materials underlay northwest and southwest axis of the study area with resistivity values ranging from 400 to approximately 6000 m in blue, yellow, red, and green, which could indicate coarse, medium, and fine sand. As illustrated in Figure 2h, low resistivities values were found in the northeast section of the research region, with resistivities ranging from 0 to about 400 m in purple, which could imply clay/shale. At AB/2 at 15 m, the purple color covers a considerable portion of the iso-resistivity (Figure 2h).

4.12 Iso-resistivity map (AB/2 at 15 m repeated)

When comparing the AB/2 contour map of iso-resistivity strength at 15 m to AB/2 at 15 m, the trend of resistivity showed a modest decrease in resistivity. Figure 2i shows relative high resistive materials underlay the SW, SE, and SE of the study area in red, blue, and green, with resistivity values ranging from 400 to approximately 5000 m, possibly interpreted as area underlain by coarse, medium, and fine sand, and yellow selected part of NE, and SE in purple, possibly interpreted as area underlain by sand/clay.

4.13 Iso-resistivity map (AB/2 at 20 m)

Most sections of the study area in the SW, SE, and selected parts of the NE axis are characterized by relatively high resistive materials, as seen in the AB/2 contour map of iso-resistivity strength at 20 m in Figure 2j. The study's resistivity at these sounding stations revealed that resistivity values range from 2500 to about 7500 m, with yellow, blue, and red indicating areas underlain by coarse, medium, and fine sand, respectively. Blue represents coarse, medium, and fine sand, with average resistive values ranging from 500 to approximately 2500 m.

4.14 Iso-resistivity map (AB/2 at 25 m)

The iso-resistivity strength AB/2 contour map at 25 m in Figure 2k below shows relatively high resistive materials underlying the NW axis of the study area, with resistivity values ranging from 3000 to about 7500 m in green, yellow, and red. The green, yellow, and red color ranges denote coarse, medium, and fine sand, respectively. Low resistivities values were found in the SW and SE parts of the research area, with resistivities ranging from 0 to 500 m in purple, indicating an area underlain by clay/sand.

4.15 Iso-resistivity map (AB/2 at 32 m)

The AB/2 contour map of iso-resistivity strength at 32 m in Figure 2l below shows relatively high resistive materials underlying the NW and NE parts of the figure, with resistivity values ranging from 2000 to about 6500 m in yellow, green, and red. This could indicate an area underlain by coarse, medium, and fine sand, which is consistent with research by who found that the geology of the study area is mostly sand with little shale/clay (Oomkens, 1974; Akpoborie et al., 2011; Eyankware, and Ephraim, 2021). Resistivity values of 500 to 2000 m in the blue area of Figure 2l can be interpreted as coarse, medium, and fine sand. Low resistivity values of 0 to approximately 500 m in purple color were reported in the SW and NE, which could imply clay/sand.

4.16 Iso-resistivity map (AB/2 at 40 m)

In comparison to AB/2 at 32 m, the AB/2 contour map of iso-resistivity strength at 40 m in Figure 2m below reveals a trend of resistivity values that slightly rise. The SE section of the area was underlain by rather high resistive materials, with resistivity values ranging from 2000 to around 10500 m, which may be interpreted as coarse, medium, and fine sand. Low resistive value was observed in a larger part of Figure 2m in purple with a resistivity value of 500 to approximately 1500 Ωm may indicate sand/clay.

4.17 Iso-resistivity map (AB/2 at 40 m repeated)

The AB/2 contour map of iso-resistivity strength at 40 m (repeated) in Figure 2n below revealed relatively high resistive materials underlay the NE, SW, and selected part of SE, in blue, green, yellow, and red color, with resistivity values ranging from 1000 to approximately 3600 m, which could be interpreted as coarse, medium, and fine sand. Low resistive material was found in purple in the SE, SW, and a portion of the NE, which could imply medium or fine sand (Figure 2m) with a resistance of 600 to 1000 m. It was discovered in Figure 2n that the area underlain by coarse, medium, and fine sand at AB at 40m repeated may suggest an area underlain by coarse, medium, and fine sand.

4.18 Iso-resistivity map (AB/2 at 50 m)

When comparing the AB/2 contour map of iso-resistivity strength at 50 m to AB/2 at 40 m, Figure 2o shows a resistivity value trend that is slightly lower (repeated). The NW, SW, NE, and a portion of the SE of the research region were underlain by relative high resistive materials with a resistivity value range of 900 to about 2100 m in red, blue, yellow, and green, which could be interpreted as coarse, medium, and fine sand in Figure 2 o. Low resistivity values of 700 to about 800 m were found in the SE section of the study area in purple, indicating that the area is underlain by medium to fine sand.

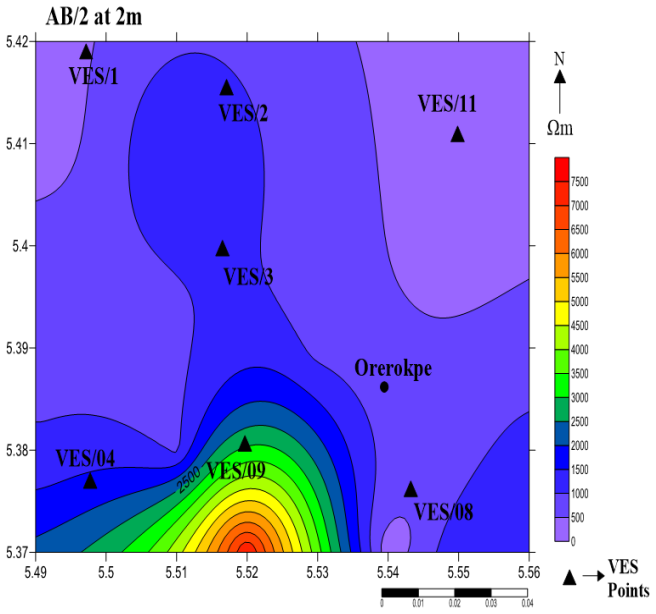

(a)

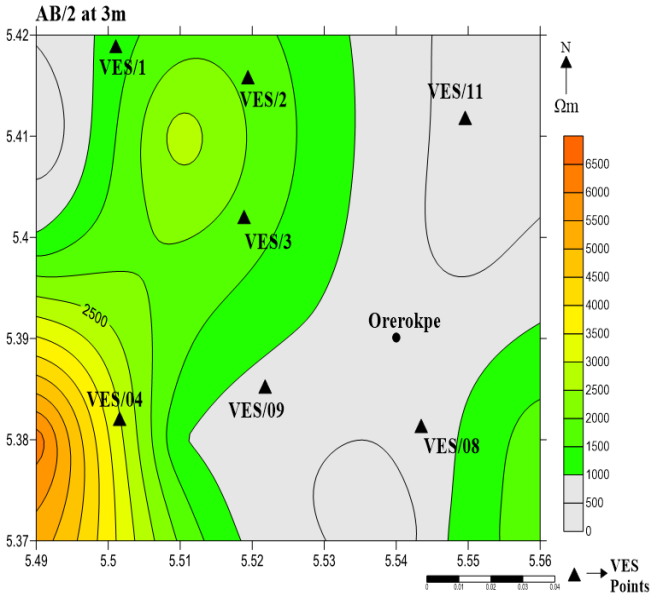

(b)

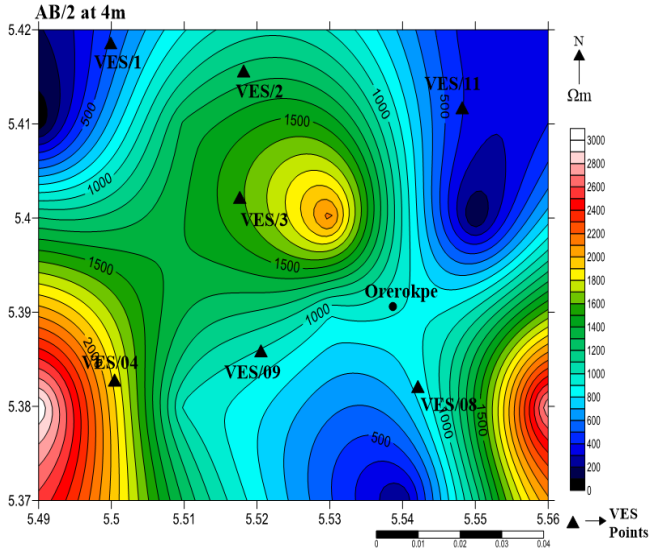
AB/2 at 4m
VES/1
VES/2
VES/3
VES/04
VES/09
VES/08
VES/11
Orerokpe
N
Ωm
VES Points

(c)

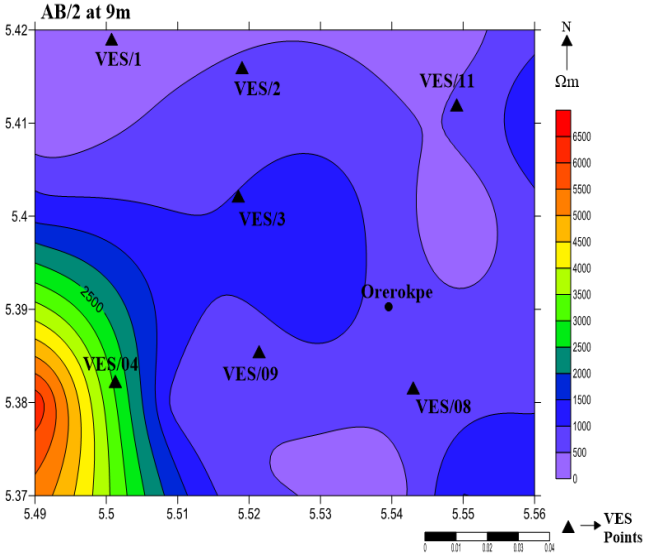
AB/2 at 9m
VES/1
VES/2
VES/3
VES/04
VES/09
VES/08
VES/11
Orerokpe
N
Ωm
VES Points

(f)

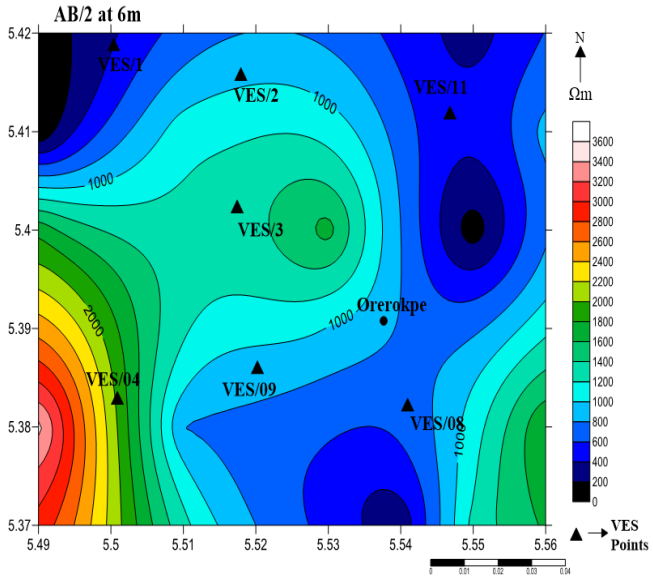
AB/2 at 6m
VES/1
VES/2
VES/3
VES/04
VES/09
VES/08
VES/11
Orerokpe
N
Ωm
VES Points

(d)

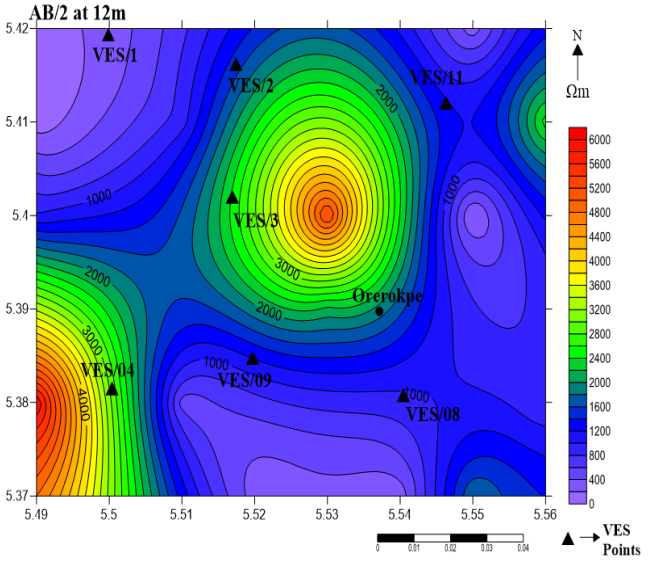
AB/2 at 12m
VES/1
VES/2
VES/3
VES/04
VES/09
VES/08
VES/11
Orerokpe
N
Ωm
VES Points

(g)

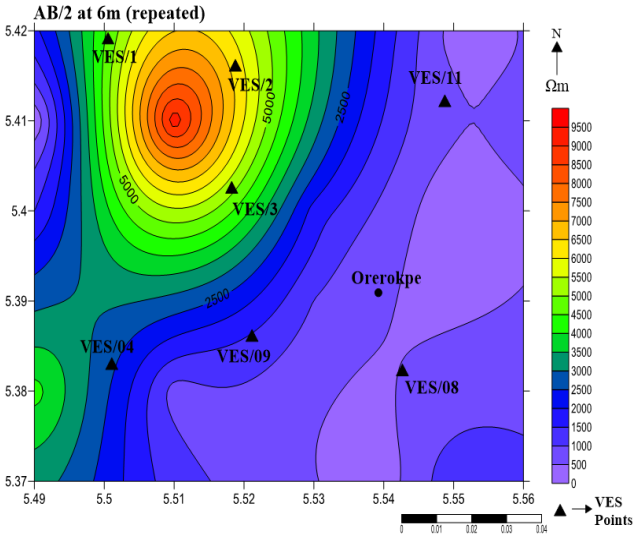
AB/2 at 6m (repeated)
VES/1
VES/2
VES/3
VES/04
VES/09
VES/08
VES/11
Orerokpe
N
Ωm
VES Points

(e)

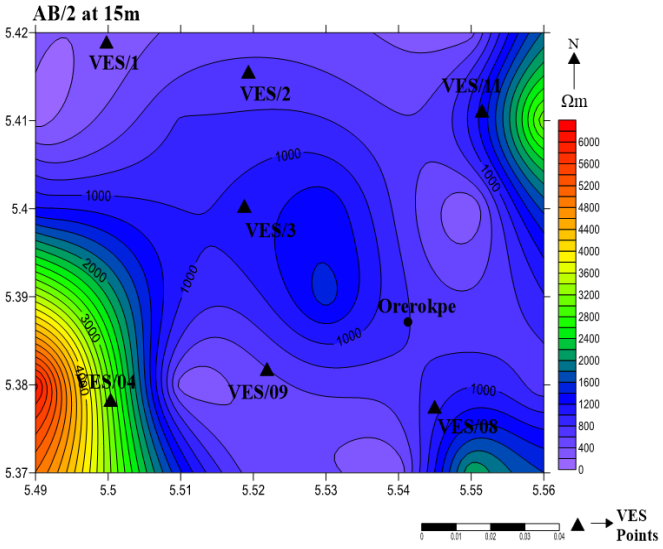
AB/2 at 15m
VES/1
VES/2
VES/3
VES/04
VES/09
VES/08
VES/11
Orerokpe
N
Ωm
VES Points

(h)

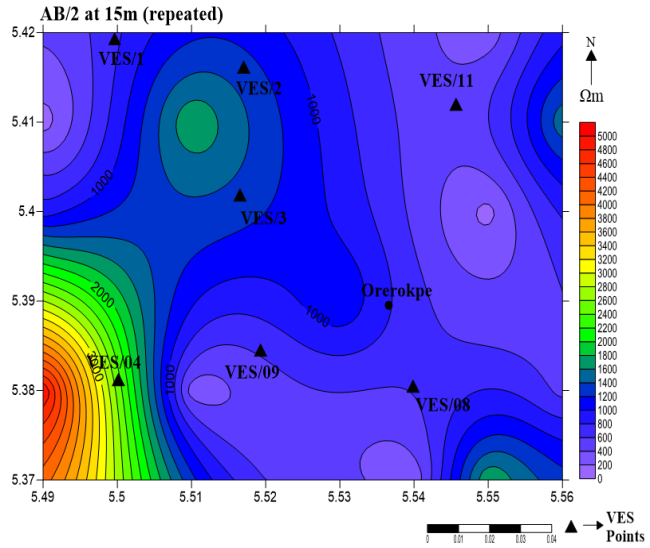
AB/2 at 15m (repeated)
VES/1
VES/2
VES/11
VES/3
Ororokpe
VES/04
VES/09
VES/08
N
Ωm
VES Points

(i)

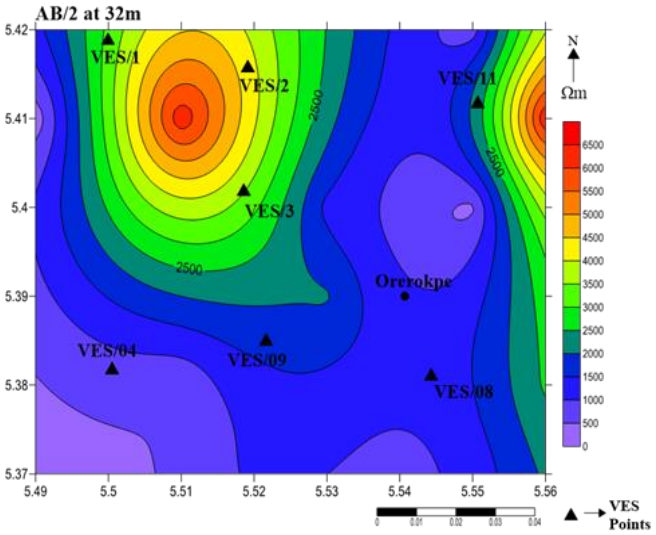
AB/2 at 32m
VES/1
VES/2
VES/11
VES/3
Ororokpe
VES/04
VES/09
VES/08
N
Ωm
VES Points

(l)

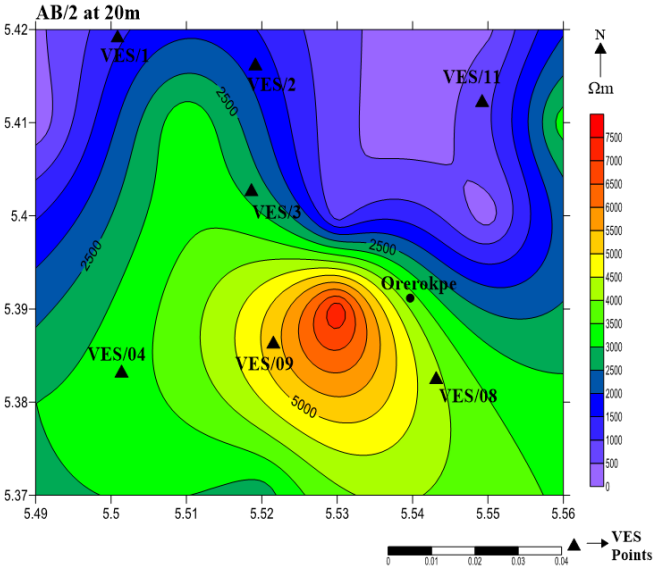
AB/2 at 20m
VES/1
VES/2
VES/11
VES/3
Ororokpe
VES/04
VES/09
VES/08
N
Ωm
VES Points

(j)

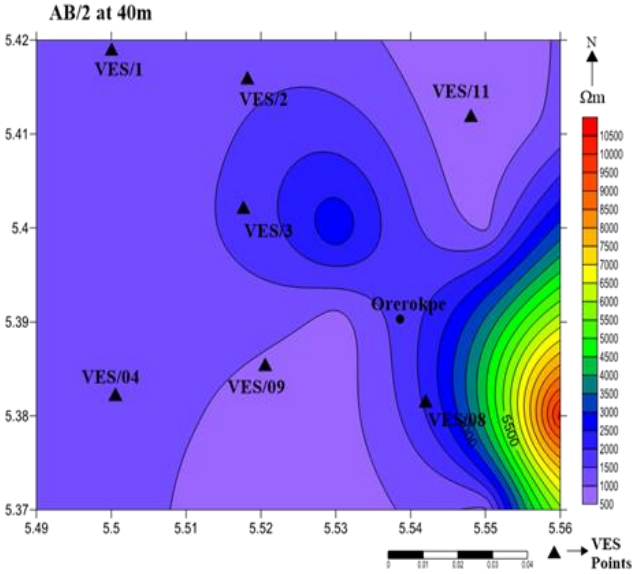
AB/2 at 40m
VES/1
VES/2
VES/11
VES/3
Ororokpe
VES/04
VES/09
VES/08
N
Ωm
VES Points

(m)

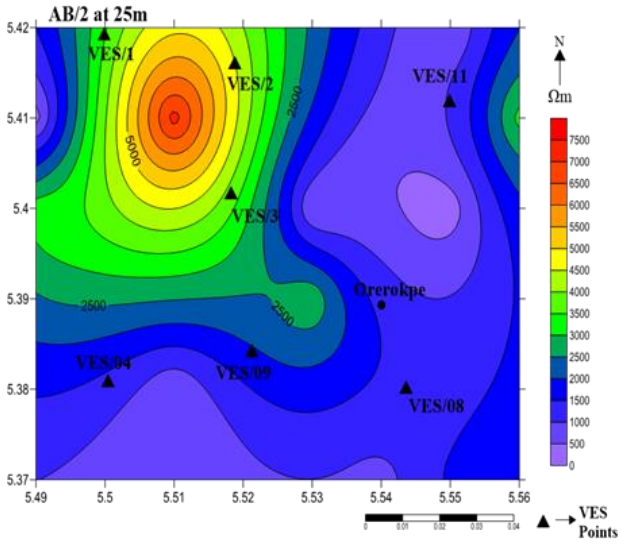
AB/2 at 25m
VES/1
VES/2
VES/11
VES/3
Ororokpe
VES/04
VES/09
VES/08
N
Ωm
VES Points

(k)

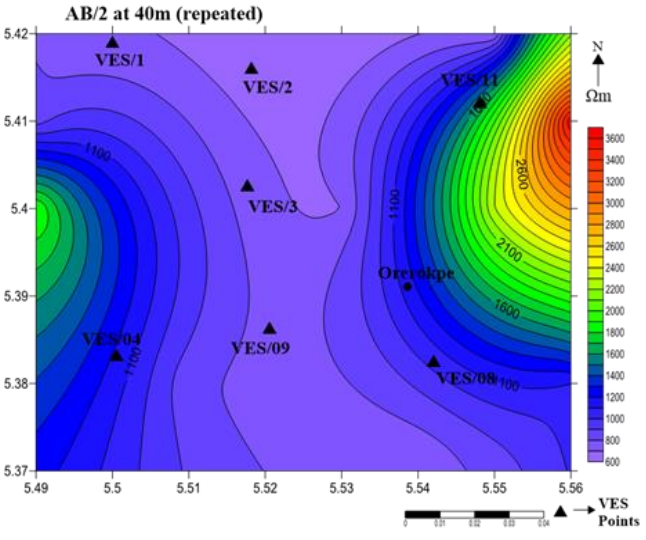
AB/2 at 40m (repeated)
VES/1
VES/2
VES/11
VES/3
Ororokpe
VES/04
VES/09
VES/08
N
Ωm
VES Points

(n)

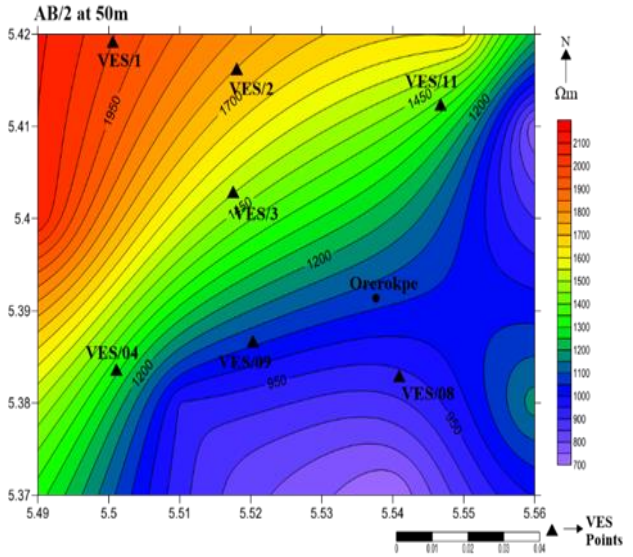

(o)

Figure 2: Contour map of the iso-resistivity values across study area: 2 a 2 m, 2b 3 m, 2 c 3 m, 2d 4 m, 2e 6 m, 2f 6 m (repeated), 2g 9 m, 2 h 12 m, 2i 15 m, 2 j 15 m (repeated 20 m, 2 k 25 m, 2l 32 m, 2 m 40 m, 2 n 40 m (repeated), and 2o 50 m.

5. Conclusion

Fifteen (15) Vertical Electrical Soundings (VES) was used to delineate the subsurface lithology to a depth of about 200 m. A correlation of VES to drilled borehole data suggested that the Orerokpe is underlain by clay, coarse, medium, and fine sand respectively with varying resistivity values. Findings from iso-resistivity plots suggested that as AB/2 increase with depth the study area is underlain by sand. Further findings suggested clay as underlying lithology was last observed at AB/2 at 32m, AB/2 at 40 m – 50m the study area was underlain by sand. At a depth of AB/2 at 40m - 50m sand can be mined at economically quantity. Moreso, residential homes and other structure within the study area is prone to land sliding. Further geotechnical study is recommended before building of houses and other structures to avoid future collapse of buildings. Application of integrated geophysical methods is recommended for better description of subsurface lithology.

References

Ajayi, O., Olorunfemi, M.O., Ojo, J.S., Adegoke-Anthony, C.W., Chikwendu, K.K., Oladapo, M.I., Idornigie, A.I., Akinluyi, F., 2005. Integrated geophysical and geotechnical investigation of a damsite on river Mayo Ini, Adamawa State, northern Nigeria. Afr Geosci Rev., 12 (3), Pp. 179–188.

Akpoborie, I.A., Ekakite, O.A., Adaikpoh, E.O., 2000. The Quality of Groundwater from Dug Wells in Parts of the Western Niger Delta. Knowledge Review, 2 (5), Pp. 72-75.

Akpoborie, I.A., Nfor, B., Etobro, A.A.I., Odagwe, S., 2011. Aspects of the geology and groundwater conditions of Asaba, Nigeria. Archives of Applied Science Research, 3 (2), Pp. 537- 550.

Alile, M.O., Amada sun, C.V.O., Evbuomwan, A.I., 2008. Application of Vertical Electrical Sounding Method to Decipher the Existing Subsurface Stratification and Groundwater Occurrence Status in a Location in Edo North of Nigeria. International Journal of Physical Sciences, 3 (10), Pp. 245-249.

Allen, J.R.L., 1965. Late Quaternary Niger Delta and Adjacent Areas: Sedimentary Environments and Lithofacies. Bulletin American Association of Petroleum Geology, 49 (5), Pp. 547–600.

Allen, J.R.L., 1970. Sediments of the modern Niger delta: A Summary and Review, In: J. P. Morgan, (ed.) Deltaic Sedimentation: Special Publications of the Society of Economic Paleontologists and Mineralogists, Tulsa, OK, 15, Pp. 138-151.

Amajor, L.C., 1990. Aquifers in the Benin Formation (Miocene Recent), Eastern Niger Delta, Nigeria: Lithostratigraphy, Hydraulics, and Water Quality. Environmental Geology and Water Science, 17 (2), Pp. 85-101.

Aweto, K.E., 2013. Resistivity methods in hydro-geophysical investigation for groundwater in Aghalokpe, Western Niger Delta. Global Journal of Geological Science, 11, Pp. 47-55

Aweto, K.E., Akpoborie, I.A., 2015. Estimating Aquifer Parameters with Geoelectric Soundings: Case Study from the Shallow Benin Formation at Orerokpe, Western Niger Delta, Nigeria. British Journal of Applied Science & Technology, 6 (5), Pp. 486-496.

Chukwuma, E.C., Orakwe, L.C., Anizoba, D.C., Amaefule, D.O., Odoh, C.C., Nzediegwu, C., 2015. Geo-electric Groundwater vulnerability assessment of overburden aquifers at Awka in Anambra State, South-Eastern Nigeria. European Journal of Biotechnology and Bioscience, 3 (1), Pp. 29-34.

Durotoye, B., 1989. Quaternary Sediments in Nigeria, In: C.A. Kogbe (ed.) Geology of Nigeria, Rockview, Jos., Pp. 431-444

Ebong, D.E., Anthony, E.A., Anthony, A.O., 2014. Estimation of geo-hydraulic parameters from fractured shales and sandstone aquifers of Abi (Nigeria) using electrical resistivity and hydrogeologic measurements. Journal of African Earth Sciences, 96, Pp. 99-109.

Edet, A.E., Okereke, C.S., 1997. Assessment of hydrogeological conditions in basement aquifers of the Precambrian Oban Massif, southeastern Nigeria. J.A. Geophy., 36 (4), Pp. 195–204. doi:10.1016/S0926-9851(96)00049-3

Eduvie, M.O., 2002. Hydro-geological geophysical evaluation of groundwater resources of the Gundumi formation and around Daura, Northwestern Nigeria, Water Resources. Journal of Nigeria Association of Hydrogeologist (NAH), 13, Pp. 46-49.

Eyankware, M.O., 2015. Estimation of Aquifer Parameters Using Geoelectrical sounding in Ochudo City, Abakaliki Ebonyi State Southeastern Nigeria. 27th Annual Nigerian Association of Hydrogeologists Conference.

Eyankware, M.O., 2019. Integrated Landsat Imagery and Resistivity Methods in Evaluation of Groundwater Potential of Fractured Shale at Ejekwe Area, Southeastern Nigeria, Unpublished PhD Thesis

Eyankware, M.O., Akakuru, C.O., Eyankware, E.O., 2022. Hydrogeophysical delineation of aquifer vulnerability in parts of Nkalagu areas of Abakaliki, SE. Nigeria. Sustainable Water Resources Management, https://doi.org/10.1007/s40899-022-00603-6.

Eyankware, M.O., Aleke, G., 2021. Geoelectric investigation to determine fracture zones and aquifer vulnerability in southern Benue Trough southeastern Nigeria. Arabian Journal of Geosciences, 2021. https://doi.org/10.1007/s12517-021-08542-w

Eyankware, M.O., Ephraim, B.E., 2021. A comprehensive review of water quality monitoring and assessment in Delta State, Southern Part of Nigeria. Journal of Environmental & Earth Science, 3 (1), Pp. 16–28. https://doi.org/10.30564/jees.v3i1.2900

Eyankware, M.O., Ogwah, C., Selemo, A.O.I., 2020. Geoelectrical parameters for the estimation of groundwater potential in fracture aquifer at sub-urban area of Abakaliki, SE Nigeria. International Journal of Earth Science and Geophysics, 6, Pp. 031. https: //doi:10.35840/2631-5033/1831

Eyankware, M.O., Ogwah, C., Umayah, O.S., 2021. Integrated geophysicaland hydrogeochemical characterization and assessment of groundwater vulnerability in Adum West Area of Benue State, Nigeria. J. Geol. Res., 65, Pp. 6588128. https://doi.org/10.30564/jgr.v3i3.3197

Eyankware, M.O., Umayah, S.O., 2022. 1D modeling of aquifer vulnerability and soil corrosivity within the sedimentary terrain in Southern Nigeria, using resistivity method. World News of Natural Science, 41, Pp. 33-50.

Mbonu, P.D.C., Ebeniro, J.O., Ofoegbu, C.O., Ekine, A.S., 1991. Geoelectric sounding for the determination of aquifer characteristics in parts of the Umuahia area of Nigeria. Geophysics, 56 (2), Pp. 284-291.

Nigerian Meteorological Agency. 2003. Warri Meteorological Bulletin. In: National Meteorological Report.

Odemerho, F.O., Ejemeyovwi, D.O., 2007. The Physiographic Provinces and Drainage Systems of Delta State, Nigeria, In: F.O. Odemerho et al.(eds) Delta State in Maps, Delta State University, Abraka. Pp. 9-17.

OIi, I.C., Ahairakwem, C.A., Opara, A.I., Ekwe, A.C., Osi-Okeke, I., Urom, O.O., Udeh, H.M., Ezennubia, V.C., 2020. Hydrogeophysical assessment and protective capacity of groundwater resources in parts of Ezza and Ikwo areas, southeastern Nigeria. Int J Energy Water Resour. https://doi.org/10.1007/s42108-020-00084-3

Olorunfemi, M.O., Fasuyi, S.A., 1993. Aquifer types and the geoelectric/hydrogeologic characteristics of part of the central basement terrain of Nigeria (Niger State). J. Afr. Earth Sci., 16 (3), Pp. 309–317. doi:10.1016/0899-5362(93)90051-Q.

Olorunfemi, M.O., Fatoba, J.O., Ademilua, L.O., 2005. Integrated VLF-electromagnetic and resistivity survey for groundwater in a crystalline basement complex terrain of southwest Nigeria. Global J. Geol. Sci., 3 (1), Pp. 71–80.

Oomkens, E., 1974. Lithofacies relations in the late quaternary Niger Delta Complex. Sedimentology, 21, Pp. 195-222.

Orellana, E., Mooney, H.M., 1966. Master tables and curves for vertical electrical sounding over layered structures. Inerciencia-Costanilla de Los Angeles, Los Angeles, Pp. 125.

Rilwanu, T.Y., 2014. Assessment of groundwater potential for rural water supply in parts of Kano State, northern 378 Nigeria. unpublished Ph. D thesis submitted to the Department of Geography, Ahmadu Bello University, Zaria.

Short, K.C., Stauble, A.J., 1967. Outline of Geology of Niger Delta. AAPG Bulletin, 51, Pp. 761-779

Umayah, O.S., Eyankware, M.O., 2022. Aquifer evaluation in southern parts of Nigeria from geo-electrical derived parameters. World News of Natural Science, 42, Pp. 28-43.